Analysis of Various Sequence-Specific Triplexes by Electron and Atomic Force Microscopies

Dimitry I. Cherny,*# Alain Fourcade,# Fedor Svinarchuk,¶‖ Peter E. Nielsen,§ Claude Malvy,¶ and Etienne Delain#

*Institute of Molecular Genetics, 123182 Moscow, Russia; #Laboratoire de Microscopie cellulaire et moléculaire, URA 147 du CNRS, Institut Gustave-Roussy, F-94805 Villejuif, France; §Department of Biochemistry B, The Panum Institute, DK-2200 Copenhagen N, Denmark; ¶Laboratoire de Biochimie-enzymologie, URA 147 du CNRS, Institut Gustave-Roussy, F-94805 Villejuif, France; and ‖Department of Biochemistry, Novosibirsk Institute of Bioorganic Chemistry, Novosibirsk 630090, Russia

ABSTRACT Sequence-specific interactions of 20-mer G,A-containing triple helix-forming oligonucleotides (TFOs) and bis-PNAs (peptide nucleic acids) with double-stranded DNA was visualized by electron (EM) and atomic force (AFM) microscopies. Triplexes formed by biotinylated TFOs are easily detected by both EM and AFM in which streptavidin is a marker. AFM images of the unlabeled triplex within a long plasmid DNA show a ~0.4-nm height increment of the double helix within the target site position. TFOs conjugated to a 74-nt-long oligonucleotide forming a 33-bp-long hairpin form extremely stable triplexes with the target site that are readily imaged by both EM and AFM as protruding DNA. The short duplex protrudes in a perpendicular direction relative to the double helix axis, either in the plane of the support or out of it. In the latter case, the apparent height of the protrusion is ~1.5 nm, when that of the triplex site is increased by 0.3–0.4 nm. Triplex formation by bis-PNA, in which two decamers of PNA are connected via a flexible linker, causes deformations of the double helix at the target site, which is readily detected as kinks by both EM and AFM. Moreover, AFM shows that these kinks are often accompanied by an increase in the DNA apparent height of ~35%. This work shows the first direct visualization of sequence-specific interaction of TFOs and PNAs, with their target sequences within long plasmid DNAs, through the measurements of the apparent height of the DNA double helix by AFM.

INTRODUCTION

The sequence-specific recognition of dsDNA by proteins plays a central role in many cellular events such as transcription, replication, recombination, packaging, and topological manipulations. During the last decade numerous attempts have been made to use oligonucleotides, particularly triple-helix-forming oligonucleotides (TFOs) (Beal and Dervan, 1991; Hélène, 1991; Thuong and Hélène, 1993), and, lately, peptide nucleic acids (PNAs) (Nielsen et al., 1994; Knudsen and Nielsen, 1996) as tools for exploring DNA structure and for creating methods for regulation of gene expression and genome analysis. TFOs and PNAs form triplexes with DNA, albeit of a different nature. The stability of the triplexes and the efficiency of their formation are significantly affected by 1) the nature and the concentration of mono and divalent cations, pH, and temperature; 2) the triplex structure and base composition; and 3) the length of the ligand.

Conventional transmission electron microscopy (EM) has proved to be an efficient method for the study of TFO and PNA triplexes. For example, we have shown that sequence-specific DNA binding of TFOs of various lengths and composition can be detected by conventional transmission EM using biotinylated derivatives of TFOs and streptavidin as a marker of triplex formation (Cherny et al., 1993b, 1994; Svinarchuk et al., 1996). This was shown for canonical PuPyPu and PyPyPy triplexes formed by TFOs 14–20 nt long. Recently we also demonstrated the EM detectability of weak alternate-strand triplexes formed by 11-mer G,T-containing oligonucleotide tagged with an intercalating chromophore (Bouziane et al., 1996). Long pyrimidine·purine tracts several tens of base pairs in length can be detected by EM directly via triplex formation without any additional labeling (Lee et al., 1995).

Selective interaction of PNA with double-stranded DNA results in the formation of highly stable PNA_2/DNA triplex with the complementary DNA strand, resulting in a P-loop (Nielsen et al., 1991, 1994). For the particular case of a long target $(dA)_{98}/(dT)_{98}$ and PNA H-T_{10}-LysNH_2, binding occurs along the whole length of the target and can be directly monitored by EM as a loop (Cherny et al., 1993a). Interaction with short target sites (e.g., 10 bp) can be visualized by using biotinylated PNA combined with streptavidin as a marker of the binding (Demidov et al., 1994).

Likewise, triplex formation can be followed by scanning probe microscopy techniques. In particular, it was reported that atomic force microscopy (AFM) is able to detect short triplexes by using biotinylated derivatives of TFO labeled with streptavidin-gold or streptavidin-alkaline phosphatase conjugates (Pfannschmidt et al., 1996). Putative long triple-stranded DNA segments formed either by poly(dA) and poly(dT) or poly(dG) and poly(dC) can be revealed without

Received for publication 22 May 1997 and in final form 4 November 1997.

Address reprint requests to Dr. Dimitry I. Cherny or Dr. Etienne Delain, Laboratoire de Microscopie Cellulaire et Moléculaire, URA 147 du CNRS, Institut Gustave-Roussy, rue Camille Desmoulins, F-94805 Villejuif, France. Dr. Delain: Tel.: 33-1-42-11-4876; Fax: +33-1-42-11-5276; E-mail: edelain@igr.fr. Dr. Cherny: Fax: +7-095-1960221; E-mail: dtcherny@img.ras.ru.

0006-3495/98/02/1015/09 $2.00

any additional marker, just by measuring the apparent height of the DNA filaments (Hansma et al., 1996).

To obtain a faithful triplex detection by EM or AFM, allowing their use in the mapping of short nucleotide sequences in DNA molecules via triplex formation, a control of the experimental conditions of the DNA samples preparation is needed. For example, these conditions should not influence the triplex stability or the efficiency of its detection. In particular, one seeks conditions for stabilizing triplexes without impairing their sequence selectivity. The efficiency of regular triplex detection is often less than that expected from theoretical prediction. This effect depends mainly on triplex stability, the particular structure of TFOs in solution (Svinarchuk et al., 1996), and presumably, conditions of sample preparation for microscopy. PNA_2/DNA triplexes can also be detected by EM, although at a lower efficiency relative to that determined by gel retardation experiments (Demidov et al., 1994).

Researchers using AFM techniques have adopted an ancient EM procedure for imaging DNA molecules, i.e., adsorption to the surface of freshly cleaved mica in the presence of magnesium ions (Brack, 1981). Despite the fact that the resolution of the biological objects by AFM has not achieved its full potential and is still inferior to that of EM (Delain et al., 1992a; Hansma et al., 1995; Larquet et al., 1996; Pfannschmidt et al., 1996), AFM observation has some advantages over EM. It reveals the topography of the object or, in a stricter sense, the topography of the object subjected to its interaction with the scanning tip. More, complexes of DNA with sequence-specific bound ligands can be directly detected by AFM via their coupling with small proteins that cannot be seen directly in EM. Last, AFM can imaged under liquid (Hansma et al., 1993, 1995; Schaper et al., 1994; Lyubchenko and Shlyakhtenko, 1997); this has not yet been fully explored for biological objects and triplexes in particular. Moreover, the direct adsorption of molecules to mica is less convenient for EM, because it requires the preparation of metal-decorated carbon replicas for the observation. The differences in the EM and AFM procedures for sample preparation may have important effects on the structure of the observed complexes. Thus it is important to make comparative observations using both EM and AFM, to understand and eventually minimize the influence of the preparation procedures on the conformation of the molecules.

Here we present new data on the imaging by both EM and AFM, of various triplexes formed by G,A-containing TFOs and bisPNAs. The complementarity of the approaches in studying these complexes is demonstrated.

MATERIALS AND METHODS

Preparation of canonical triplexes

The oligonucleotide 5′-GGAGGAGGAGGAGGGGGAGG-3′-biotin (bio-VPX20) was purchased from GenSet (Paris, France). The plasmid pVpx1 containing the polypurine stretch of the SIV *vpx* gene was made by inserting the oligonucleotide 5′-CTAGACCTGGAGGGGGAGGAG-GAGGAGGTCCG-3′/5′-GATCCGGACCTCCTCCTCCTCCCCCTCC-AGGT-3′ into the *Xba*I-*Bam*HI sites of the vector pBluescript II (Stratagene, La Jolla, CA). Plasmid was purified as described by Svinarchuk et al. (1996). Triplex was obtained by a procedure similar to that previously described (Cherny et al., 1993b; Svinarchuk et al., 1996): 0.3–2 μg of DNA was incubated with the bio-VPX-20 in a 10-μl volume containing 10 mM Tris-HCl (pH 7.5), 50 mM NaCl, or 150 mM KCl (where indicated), 10 mM $MgAc_2$ for 1.5–2 h at 37°C. The concentration of TFO was 0.75 μM. After the incubation, the mixture was passed through a Superose 6 column (Smart System, Pharmacia Biotech, Uppsala, Sweden) equilibrated with buffer containing 10 mM Tris-HCl (pH 7.5), 50 mM NaCl, and 10 mM $MgAc_2$, then streptavidin (Sigma Chemical Co., St. Louis, MO) was added to the DNA-containing fractions to a final concentration of 5–20 μg/ml (80–300 nM); after a 10-min incubation at room temperature, the gel filtration step was repeated, and DNA-containing fractions were used for EM or AFM experiments.

The oligonucleotide 5′-**GGAGGAGGAGGAGGGGGAGG**TTT-GCTGACGCAGATGTCCTAATATGGACATCCTGTTTTTTACAGG-ATGTCCATATTAGGACATCTGCGTCAGC-3′ (VPX20-stem) was synthesized on an Applied Biosystems 391 DNA synthesizer (Foster City, CA), using the solid-phase phosphoramidite procedure, and subsequently purified by polyacrylamide gel elctrophoresis. The sequence responsible for triplex formation is indicated in bold, and the sequence forming a hairpin is underlined. To augment the efficiency of triplex formation, TFO was first annealed with a 1.5 M excess of 3′-CCTCCTCCTCCT-5′ oligonucleotide matching the 5′-end of the triplex-forming sequence in a buffer containing 10 mM Tris-HCl (pH 7.5), 150 mM KCl, and 10 mM $MgAc_2$ at 90°C for 5 min, and then the mixture was allowed to slowly cool down to room temperature. Then modified TFO was incubated with the pVpx1/*Kpn*I plasmid in a 10-μl volume containing 10 mM Tris-HCl (pH 7.5), 150 mM KCl, and 10 mM $MgAc_2$; the final concentration of TFO was 0.75 μM. Then the sample was passed through a Superose 6 column equilibrated with the same buffer, and the DNA-containing fractions were used for both EM and AFM observations.

Preparation of PNA_2/DNA triplexes

PNA H-TTJTTJTTTT-Lys-aha-Lys-aha-Lys-TTTTCTTCTT-LysNH_2 (PNA 554) was synthesized and purified according to the methods of Christensen et al. (1995) and Egholm et al. (1995); the biotinylated derivative bio-TTJTTJTTTT-Lys-aha-Lys-aha-Lys-TTTTCTTCTT-LysNH_2 (bioPNA, PNA 1021) was obtained as described (Demidov et al., 1994). J denotes the synthetic nucleobase pseudoisocytosine. Plasmids were obtained by cloning either one 5′-GAAGAAGAAAACTGAC sequence into the *Pst*I site of the pUC19 vector (pA8G2–1) or two of them into the *trans* position, also at the *Pst*I site (pT8C2–2), and purified as described by Nielsen et al. (1993). A small *Pvu*II-*Pvu*II fragment of each plasmid DNA containing the target sequence(s) was used. The fragments were purified on a MonoQ column (Smart System; Pharmacia Biotech).

Triplexes were obtained by incubation in a 10-μl volume of 0.2–0.5 μg of DNA fragment with PNA in 10 mM Tris-HCl (pH 7.4), 1 mM EDTA at 37°C for 1.5–2 h; the final concentration of PNA varied from 2 μM to 10 μM. Then the mixture was passed through a Sepharose 6 column equilibrated with 10 mM Tris-HCl (pH 7.4), 50 mM NaCl and DNA-containing fractions were collected and used for EM and AFM observations. For visualization of the triplex formed by bioPNA, streptavidin was further added after the first gel filtration step to a final concentration of 5–20 μg/ml (80–300 nM), and after a 10-min incubation at room temperature the gel filtration step was repeated.

Electron microscopy

Usually a 5-μl aliquot containing 1–3 μg/ml of DNA in 10 mM Tris-HCl (pH 7.4), 50 mM NaCl, and 5–10 mM $MgCl_2$ was applied to a carbon film glow-discharged in the presence of pentylamine vapors according to the method of Dubochet et al. (1971). PNA/DNA triplexes were adsorbed

without $MgCl_2$. The samples were stained with 0.5–1% aqueous uranyl acetate for 10 s and blotted with a filter paper. Complexes with streptavidin were visualized after rotary shadowing with tantalum/tungsten with the electron gun of a Balzers MED 010 apparatus (Balzers, Balzers, Lichtenstein). The samples were observed with a Zeiss/LEO CEM-902 electron microscope (Zeiss/LEo, Oberkochen, Germany) in the annular dark-field mode as described (Dubochet, 1973; Delain et al., 1992b; Delain and Le Cam, 1995). Image recording and measurements of DNA molecules were performed with the built-in Kontron image analyzer system and software.

Atomic force microscopy

The incubation mixture was diluted to a final DNA concentration of ~1–3 μg/ml in a buffer containing 10 mM Tris-HCl (pH 7.4), 50 mM NaCl, and 5–10 mM $MgCl_2$. Three to five microliters was placed on a freshly cleaved mica surface for 30–60 s, which was washed with a few drops of 0.2% aqueous uranyl acetate, blotted intensively with filter paper, and dried under vacuum for 15–20 min. The samples were scanned with a NanoScope III (Digital Instruments, Santa Barbara, CA) in the Tapping mode in air, using standard TESPW silicon tips.

RESULTS

Visualization of regular triplex

Previously it was shown that the 20-mer G,A-containing oligonucleotide 5′-GGAGGAGGAGGAGGGGGAGG-3′ forms an extremely stable triplex with the target sequence in the presence of $MgCl_2$ (Svinarchuk et al., 1995). A 3′-biotinylated derivative also makes stable complexes with the target site, which are easily detected by EM via coupling with streptavidin (Fig. 1). Streptavidin molecules localizes either at 216 ± 15 bp (mean ± SD, 60 molecules) from one end of the smallest *Pvu*II-*Pvu*II fragment of the pVpx plasmid DNA or at 82 ± 15 bp (mean ± SD, 50 molecules), also from the nearest end of the *Kpn*I linearized DNA. These positions coincide well with those of the target sequence localized either at 195–215 bp or 66–86 bp, respectively. It is worth noting that the position of the TFO 3′ end coupled with biotin is actually positioned at 215 bp and 86 bp, respectively. Kinetic parameters of the interaction were found to be similar for both nonbiotinylated and biotinylated forms of TFO, thus indicating that the presence of biotin at the 3′ end does not have any inhibitory effect on triplex formation (Svinarchuk et al., 1996).

AFM studies of the triplex deposited on mica revealed a streptavidin positioning on the linearized pVpx/*Kpn*I DNA, very close to that determined by EM, and show comparable efficiency (Fig. 2). Streptavidin molecules are seen as large globes over the DNA molecules with an apparent diameter of up to ~15 nm and a height close to ~3 nm. The apparent height of free DNA molecules varies from 0.5 nm to 0.9 nm within each experiment, which is in good agreement with other observations (Hansma et al., 1996; Pfannschmidt et al., 1996).

Imaging of the complexes formed without adding streptavidin shows that a few DNA molecules have an increased height in the region of the target sequence (Fig. 3). We interpret this ~0.4-nm height increase as a result of the presence of the triplex.

AFM imaging of triplexes, formed with supercoiled DNA molecules and using streptavidin as a marker, clearly demonstrates the ability of the method to detect the complex (Fig. 4), whereas the EM analyses of the stained or shadowed molecules do not permit clear identification of streptavidin. Streptavidin globes have practically the same sizes as those on linear molecules. A strong dependence of triplex formation efficiency on ionic conditions was previously shown for linear molecules: replacing 50 mM NaCl in the incubation mixture with 150 mM KCl decreased the yield of the complexes from 70% to 15–20% (Svinarchuk et al., 1996). In the present case more than 90% of supercoiled molecules bear a streptavidin molecule, irrespective of the nature of the monovalent cations.

Visualization of regular triplex obtained by a TFO tagged with a 74-nt sequence-forming hairpin

In the next experiments we used the same 20-mer G,A-containing TFO 3′-tagged to the 74-nt sequence (VPX20-stem) forming a 33-bp-long hairpin by itself. There is no homology between this extra sequence and the sequence neighboring the target site. To augment the efficiency of triplex formation, VPX20-stem was first annealed to the 3′-CCTCCTCCTCCT-5′ nucleotide matching the 5′-end of the TFO recognition sequence. This was done to prevent possible inter- and intramolecular interactions of the TFO sequence itself, according to our previous observations (Svinarchuk et al., 1996). The triplex is clearly detected as a short DNA fragment attached to the long plasmid DNA (Fig. 5). The measured length of the protruded DNA is equal to 29 ± 4 bp (mean ± SD, 45 molecules) and very close to the hairpin length of 33 bp. It localizes at 85 ± 6 bp (mean ± SD, 45 molecules) from the nearest end of the plasmid DNA, which fits well with the position of the last nucleotide of the TFO-recognition sequence at the 3′ end (86 bp). No other protrusions could be found over the whole length of the plasmid DNA. At least 80% of DNA molecules have such protrusions, indicating that the efficiency of triplex formation cannot be less than this value. Protruding DNA is often seen in a perpendicular direction with respect to the DNA axis and is perceived as lying on the carbon film surface. Few molecules appeared with very short protrusions with lengths close to the EM image resolution. Presumably the main reason for this is that the protruding DNA is not lying in the plane of the carbon film, but rather is in a direction perpendicular to its surface, which does not allow an optimal visualization (see below).

AFM examination clearly demonstrates the occurrence of the protruding DNA in a correct position (Figs. 6 and 7). Likewise, protruding DNA is seen in a perpendicular direction with respect to the plasmid DNA axis. It was found that the short duplex protrudes in various directions, either in the plane (Fig. 6) or out of the plane (Fig. 7). In the former case the length of the protruding DNA is close to the expected value of 10 nm, whereas in the latter case the apparent height of the protrusion is only ~1.5 nm.

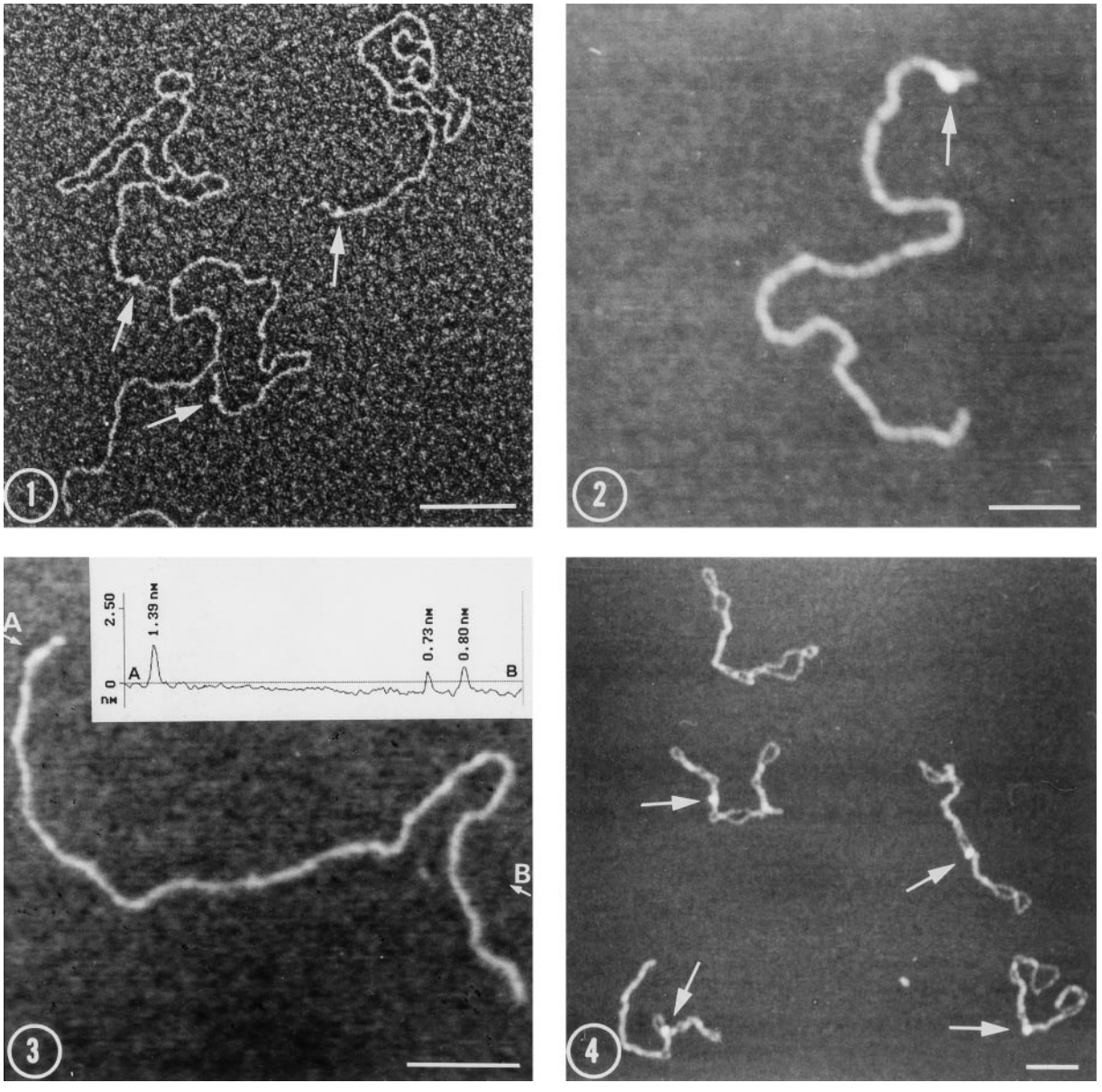

FIGURE 1 Figs. 1–4. Visualization of the triplex formed by the biotinylated 20-mer G,A-containing TFO with pVpx1 plasmid DNA in linear (Figs. 1–3) and supercoiled (Fig. 4) forms. Triplex with linear DNA was prepared in the presence of 50 mM NaCl, whereas that with supercoiled DNA was prepared in the presence of 150 mM KCl. Fig. 1, EM view; Figs. 2–4, AFM views. Triplex formation was detected via streptavidin (shown by *arrows* in Figs. 1, 2, and 4). In Fig. 3, streptavidin was omitted from the reaction. (*Inset*) Profile of the cross ection through the *A–B* line on the photograph. The scale markers indicate 100 nm.

Visualization of PNA_2/DNA triplex

Previously we have demonstrated that the formation of a PNA_2/DNA triplex by homopyrimidine PNA oligomers can easily be detected by EM via streptavidin by using biotinylated derivatives of decamer PNAs (Demidov et al., 1994). Here we show that triplex formation obtained by bisPNA consisting of two PNA decamers connected via a flexible linker results in a very pronounced DNA kinking (Figs. 8–10). This is observed for DNA fragments carrying one (fragment of pA8G2–1 plasmid) or two closely located target sites in the *trans* position (fragment of pT8C2–2 plasmid). The position of the kinks obtained from the complexes formed by the pA8G2–1 fragment with PNA 554 is equal to 132 ± 6 bp (mean ± SD; see Fig. 17) from one end of the fragment and corresponds to the position of the target site located at 135–145 bp. Examination of the images showed that independently of the concentration of the PNA used, the population of DNA molecules contains two types of molecules, i.e., either without visible bending or with kinks of various values of bending. AFM examination of the PNA/DNA complexes also revealed the presence of kinks with various bend angles (Fig. 15).

A few DNA fragments with two target sites in the *trans* position have two kinks in close vicinity, thus indicating the

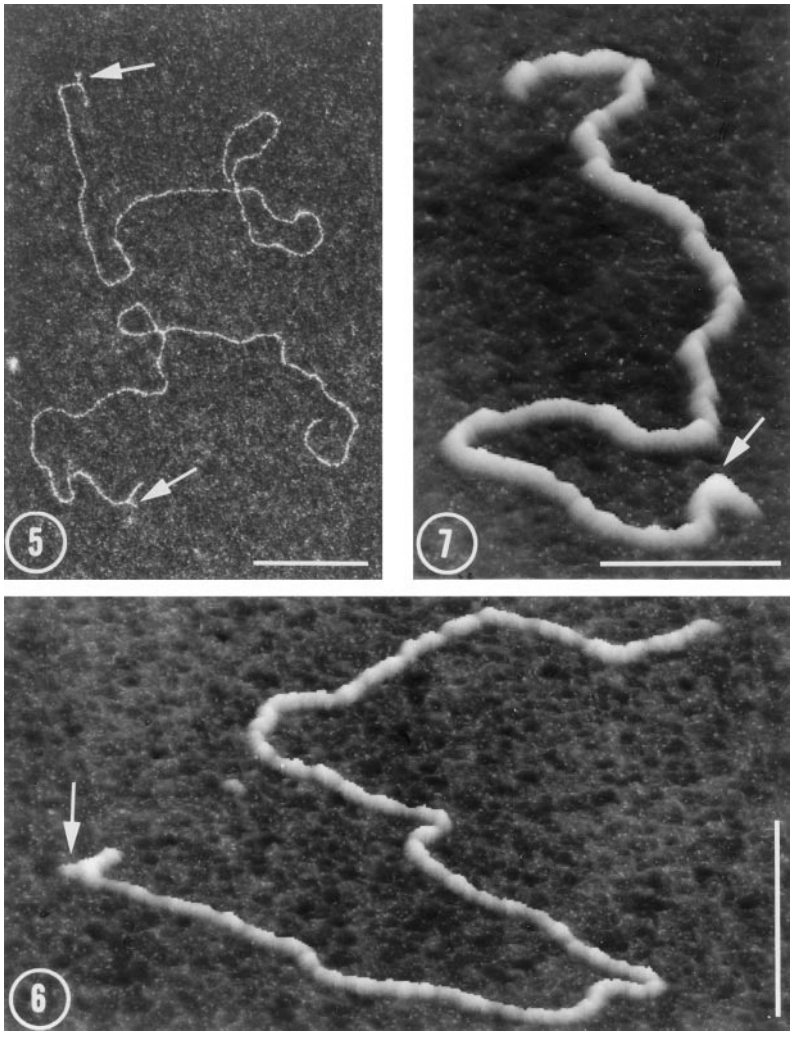

FIGURE 5 Figs. 5–7. Images of the triplex formed by the 20-mer G,A-containing TFO tagged with a 74-nt-long oligonucleotide forming hairpin with a linear form of pVpx1 plasmid DNA. Fig. 5, EM view; Figs. 6 and 7, AFM views. Protruded DNA (indicated by *arrows*) is seen as lying in the plane of imaging (Figs. 5 and 6) or out of the plane (Fig. 7). The scale markers indicate 100 nm.

presence of two neighboring PNA_2/DNA triplexes (Figs. 11 and 12). Furthermore, unusual complexes were present, with two or several DNA fragments crossing over at the position of the target site (Figs. 13 and 14). Because of the fact that PNA/DNA triplex consists of two PNA oligomers (i.e., decamers in our case), it is possible that both PNA oligomers of one bisPNA molecule may participate in triplex formation with the target sequences from different DNAs molecules, thus resulting in the appearance of cross-overed complexes.

AFM images show that for a major part of the molecules with real kinks, the height of the DNA at the kink is increased by ~35% as compared to the value for a neighboring DNA segment. The molecules without visible kinks mostly do not present any extra corrugations of the DNA axis. No correlation was found between the increase in DNA height and the value of the bend angle.

To verify whether the presence of kinks was linked to triplex formation, we prepared complexes with a biotinylated bisPNA derivative (PNA 1021) at the same concentration, using streptavidin as a marker. An electron micrograph of the complex formed with the fragment of pT8C2–2 plasmid (Fig. 16) shows that all DNA molecules have at least one streptavidin molecule located ~40% from the nearest end of the fragment, which is in good agreement with the target site positions. Most of the complexes have strong bends or kinks close to the streptavidin molecules. Few DNA fragments have two streptavidin molecules in close vicinity, thus indicating the presence of two PNA molecules. A similar pattern was also observed from the complexes of the fragment of the pA8G2–1 plasmid, with PNA 1021 either coupled or noncoupled with streptavidin. The position of the kinks was close to that of for PNA 554, whereas the position of the streptavidin molecules was found to be equal to 135 ± 15 bp (mean ± SD) from the nearest end of the DNA fragment and coincided with the position of the kinks (Fig. 17).

DISCUSSION

The results presented here demonstrate that both EM and AFM allow the detection of various types of stable triplexes formed by regular TFOs or PNAs. Usually triplexes are

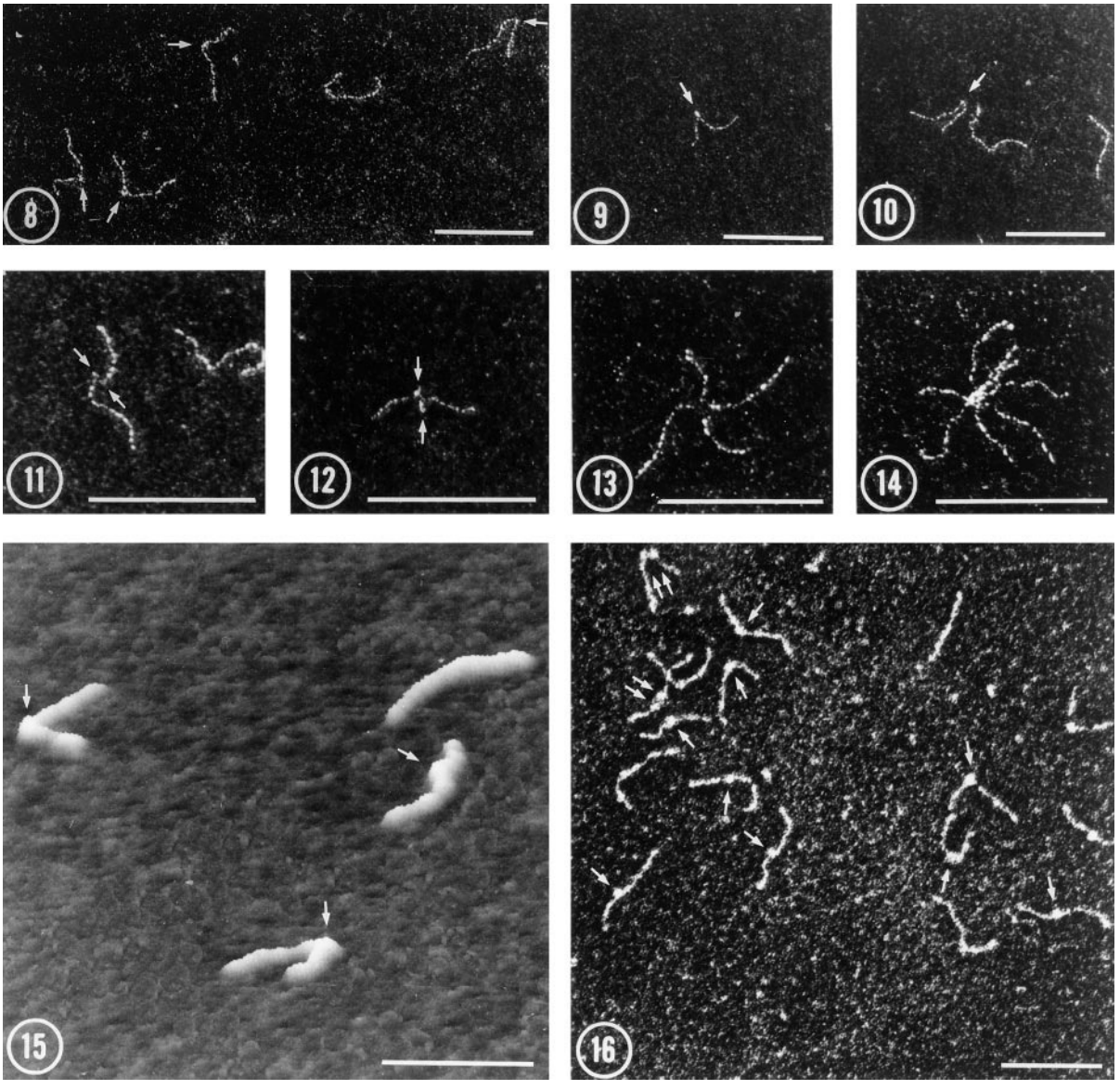

FIGURE 8 Figs. 8–16. Images of PNA_2/DNA triplex formed by bisPNA with DNA fragment carrying two target sites in the *trans* position (*Pvu*II-*Pvu*II fragment of pTC8C2–2 plasmid DNA). Figs. 8–14 and 16, EM views; Fig. 15, AFM view. Figs. 8–15 represent the triplex formed by PNA 554. Fig. 16 represents the triplex formed by bioPNA (PNA 1021) coupled with streptavidin (shown by *arrows*). Arrows in Figs. 8–15 indicate the presence of kinks in the regions or triplex formation. The scale markers indicate 100 nm.

easily detected in EM by using biotinylated derivatives of the ligands, with streptavidin as a marker. We show here that streptavidin is also a good marker for triplex detection by AFM with the same efficiency, even if it does provide an "oversize" label for this highly sensitive method of visualization. Triplexes formed by biotinylated derivatives with supercoiled DNA molecules are much more easily detected by AFM than by our usual EM procedure. In the latter case, shadowing of the samples is needed to reveal the streptavidin molecules, which are usually not visible in uranyl acetate-stained preparations imaged in the dark-field mode. The binding of a 20-mer G,A-containing TFO was more effective with supercoiled DNA as compared to linear DNA, which is in agreement with earlier observations (Svinarchuk et al., 1994). The yield of the triplexes with supercoiled DNA was close to 100%, a value that has never been reached for linear fragments. The maximum yield for the latter case did not exceed 70% under the same experimental conditions (Svinarchuk et al., 1996). Analysis of the pictures obtained both for linear and supercoiled molecules shows that triplex formed by G,A-containing 20-mer TFO does not result in any detectable change in the geometry of the DNA molecule.

AFM imaging of the regular triplex without the streptavidin marker shows that a few of the *Kpn*I-linearized DNA molecules have extra corrugations ~0.4 nm in height within the region encompassing the recognition sequence. Moreover, AFM imaging of the triplex designed by the G,A-

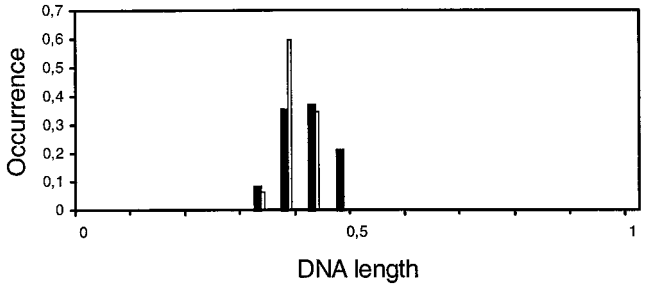

FIGURE 17 Histogram presenting the distributions of the streptavidin molecules (*filled bars*, 64 molecules) and kinks (*open bars*, 55 molecules) obtained from the complexes of the *Pvu*II-*Pvu*II fragment of pA8G2–1 plasmid with PNA 1021 and 554, respectively. Positions were plotted from the nearest end of the fragment.

containing TFO tagged with a 74-nt-long oligonucleotide also confirms an increase in DNA height by 0.3–0.4 nm. In contrast, it was reported that triplex formed by the 27-mer TFO did not result in thickening along the DNA contour (Pfannschmidt et al., 1996). These discrepancies in triplex detection can probably be explained by the small lengths of the TFOs used in these experiments, and therefore the expected corrugations would be close to the resolution limit given by the scanning tip. Long structures believed to be triple-stranded DNA formed either by poly(dA) and poly(dT) or poly(dG) and poly(dC) did show a detectable increase in their height versus double-stranded DNA (Hansma et al., 1996). The results presented here demonstrate that triple-stranded DNA does have increased height relative to that of double-stranded DNA.

Triplexes formed by the TFO 3′-tagged with a 33-bp-long hairpin are easily detected by both EM and AFM as short protruding DNA fragments, whose length (~10 nm) and position on the plasmid DNA, determined by both AFM and EM methods, coincide well with the expected values. Furthermore, the EM-determined position of the protruded DNA from the nearest end of DNA is equal to 85 ± 6 bp (mean ± SD), whereas the same TFO 5′-tagged with the same hairpin-forming sequence appeared at 70 ± 8 bp (mean ± SD, 41 molecules) from the nearest end (data not shown), which allowed determination of the TFO orientation within the triplex. It is worth noting that the target sequence is located 66–86 bp from the nearest end of DNA molecule. The apparent height of the protrusion is close to ~1.5 nm, which means that the height of the protruding DNA per se is ~0.5–0.6 nm and is markedly less than the expected value of its length (10 nm). This discrepancy is probably due to fluctuations of the hairpin, created by the tip oscillations that occur in the Tapping mode, which results in a decrease in the effective height of the protrusion.

The fact that short DNA fragments protruding out of long DNA molecules are not obligatorily lying on the surface of the mica or carbon supports is very surprising, because this requires a certain rigidity of the protruded DNA. It is worth noting that the TFO and the hairpin sequences are separated by only three bases in our case. We concluded that relatively short, strongly bent or stressed DNA segments may not necessarily stay in the plane of imaging. A similar effect has been demonstrated for minicircles of DNA, owing to the torsional stress induced by the archaebacterial histone-like protein MC1 (Larquet et al., 1996). In any case, the resulting three-dimensional structure of the complex, as well as the image, will depend on its particular structure and the DNA-support interactions, which can be detected exclusively by AFM.

Sequence-selective interaction of homopyrimidine PNA with DNA results in the formation of highly stable PNA_2/DNA triplex with one strand of the target site (Nielsen et al., 1991, 1994). BisPNAs interact more rapidly with DNA relative to monomeric ones, but still exhibit excellent sequence specificity (Kuhn et al., manuscript submitted for publication). The latter is very essential when PNA/DNA triplexes are used as markers for the detection of homopurine-homopyrimidine sequences alongside long DNA fragments by EM and AFM techniques.

The interaction of bisPNAs with the target site inserted into long plasmid DNA, linear or supercoiled, results in kinking of DNA molecules within or near the target sequence, as seen by both EM and AFM (Figs. 8–16). Analysis of the complexes formed by biotinylated PNA (PNA 1021) with the linear fragment carrying a single target site shows that for most of the molecule, the mean value of the smallest angle between two arms of DNA coming out of the streptavidin molecule is close to 110° (data not shown). On the other hand, a significant part of the molecule does not have any visible bend or kink, even at the highest PNA concentration used. This was also valid for the complexes formed by monomeric PNA (data not shown). To quantify the conformational alterations of the DNA chain upon complex formation for the whole ensemble of molecules, we measured the mean square of the end-to-end distance relative to the curvilinear distance, because this may be taken as a measure of intrinsic curvature (Wang et al., 1991; Le Cam et al., 1994). The value was equal to 0.60 ± 0.24 (mean ± SD, 501 molecules) for the original DNA fragment, whereas for that bound to PNA 1021 without coupling with streptavidin, the value was equal to 0.48 ± 0.22 (mean ± SD, 234 molecules). The difference is significant for more than 99%, as judged by *t*-test. For DNA molecules coupled with streptavidin that were taken from the same grid as that of without streptavidin the value was 0.50 ± 0.24 (mean ± SD, 300 molecules). In the latter case the level of significance is only ~30% (also judged by *t*-test), which means that there is no significant influence of streptavidin on the DNA conformation upon binding to the biotinylated PNA.

It can be argued that PNA-induced kinks do not exist in solution and are an artifact of the procedures used for imaging the complexes, particularly because of the presence of magnesium and uranyl ions. UO_2^{2+} ions (uranyl acetate in our case) are essential for positive staining of DNA molecules for EM and optional for AFM imaging. In contrast,

Mg^{2+} ions are essential for AFM imaging and optional for EM. Uranyl ion induces folding of the four-way DNA junction at a concentration of 1 mM (Møllegaard et al., 1994), which is much lower than the concentrations used in our experiments, i.e., ~50 mM and 3–5 mM for EM and AFM imaging, respectively. Magnesium ions can influence the persistence length of dsDNA; the effect is more pronounced for intrinsically curved regions (Hagerman, 1988). To check the possible effects of both ions, the following experiments were done: 1) preparing the samples for EM imaging without and in the presence of magnesium ions did not reveal any difference in kink appearance for the PNA/DNA complexes (data not shown); 2) preparing the samples for AFM imaging without uranyl acetate treatment also confirmed the presence of kinks (data not shown). Therefore, neither magnesium ions nor uranyl ions, separately or combined, are responsible for the kinks detected by EM or AFM. It is worth noting that presumably weaker structures produced by nicks were also viewed as kinks by a similar EM procedure (Le Cam et al., 1994) or cryoEM technique (Furrer et al., 1997).

According to an x-ray crystallographic structure, a PNA_2/DNA triplex is not intrinsically curved (Betts et al., 1995) and presumably is less flexible relative to duplex DNA. Therefore our data indicate that DNA bending occurs at the junction between the DNA duplex and triplex what coincides with previously reported anomalous gel mobilities of short DNA fragments strand-invaded by PNA T_{10}-Lys, interpreted in favor of the DNA bend at or near the triplex (Peffer et al., 1993). It is worth noting that one cannot exclude the possibility that an increased flexibility at the junction region, due to unstacked or partially stacked DNA bases, rather than a permanent bending, is responsible for the kinks seen by EM and AFM and the retarded migration in polyacrylamide gels (Peffer et al., 1993).

It was found that the PNA_2/DNA triplex results in a detectable increase in DNA height by ~35% of its original value, especially for the molecules with the kinks. This can be explained by the increase in geometrical diameter of the PNA_2/DNA triple helix (Betts et al., 1995) and the extruding noncomplementary DNA strand.

Dr. E. Lescot is thanked for efficient help with the oligonucleotide synthesis. Dr. C. Auclair is thanked for continuous interest in this work.

The Association for Research against Cancer (ARC) is thanked for providing funds for the atomic force microscope. This work was done in part with the help of the Programme International de Coopération Scientifique (PICS) (227 to DC) and in the framework of the International Association for the Promotion of Cooperation with Scientists from the Independent States of the Former Soviet Union (INTAS) project (94-3071).

REFERENCES

Beal, P. A., and P. B. Dervan. 1991. Second structural motif for recognition of DNA by oligonucleotide-directed triple-helix formation. *Science.* 251:1360–1363.

Betts, L., J. A. Josey, J. M. Veal, and D. R. Jordan. 1995. A nucleic acids triple helix formed by a peptide nucleic acid-DNA complex. *Science.* 270:1838–1841.

Bouziane, M., D. I. Cherny, J.-F. Mouscadet, and C. Auclair. 1996. Alternate strand DNA triple-helix-mediated inhibition of HIV-1 U5 long terminal repeat integration in vitro. *J. Biol. Chem.* 271:10359–10364.

Brack, C. 1981. DNA electron microscopy. *Crit. Rev. Biochem*. 10: 113–169.

Cherny, D. I., B. P. Belotserkovskii, M. D. Frank-Kamenetskii, M. Egholm, O. Buchardt, R. H. Berg, and P. E. Nielsen. 1993a. DNA unwinding upon strand-displacement binding of a thymine-substituted polyamide to double-stranded DNA. *Proc. Natl. Acad. Sci. USA*. 90: 1667–1670.

Cherny, D. I., A. V. Kurakin, V. N. Lyamichev, M. D. Frank-Kamenetskii, V. E. Zinkevich, K. Firman, M. Egholm, O. Burchardt, R. H. Berg, and P. E. Nielsen. 1994. Electron microscopy studies of sequence specific recognition of duplex DNA by different ligands. *J. Mol. Recognit.* 7:171–176.

Cherny, D. I., V. A. Malkov, A. A. Volodin, and M. D. Frank-Kamenetskii. 1993b. Electron microscopy visualization of oligonucleotide binding to duplex DNA *via* triplex formation. *J. Mol. Biol.* 230:379–383.

Christensen, L., R. Fitzpatrick, B. Gildea, K. H. Petersen, H. F. Hansen, T. Koch, M. Egholm, O. Buchardt, P. E. Nielsen, J. Coull, and R. H. Berg. 1995. Solid-phase synthesis of peptide nucleic acids (PNA). *J. Peptide Sci.* 3:175–183.

Delain, E., A. Fourcade, J.-C. Poulin, A. Barbin, D. Coulaud, E. Le Cam, and E. Paris. 1992a. Comparative observation of biological specimens, especially DNA and filamentous actin molecules in atomic force, tunneling and electron microscopes. *Microsc. Microanal. Microstruct.* 3:457–470.

Delain, E., A. Fourcade, B. Révet, and C. Mory. 1992b. New possibilities in the observation of nucleic acids by electron spectroscopic imaging. *Microsc. Microanal. Microstruct.* 3:175–186.

Delain, E., and E. Le Cam. 1995. The spreading of nucleic acids. *In* Visualisation of Nucleic Acids. G. Morel, editor. CRC Press, Boca Raton, FL. 35–56.

Demidov, V. V., D. I. Cherny, A. V. Kurakin, M. V. Yavnilovich, V. A. Malkov, M. D. Frank-Kamenetskii, S. H. Sonnichsen, and P. E. Nielsen. 1994. Electron microscopy mapping of oligopurine tracts in duplex DNA by peptide nucleic acid targeting. *Nucleic Acids Res*. 22: 5218–5222.

Demidov, V. V., M. V. Yavnilovich, B. P. Belotserkovskii, M. D. Frank-Kamenetskii, and P. E. Nielsen. 1995. Kinetics and mechanism of polyamide ("peptide") nucleic acid binding to duplex DNA. *Proc. Natl. Acad. Sci. USA*. 92:2637–2641.

Dubochet, J. 1973. High resolution dark-field electron microscopy. *In* Principles and Techniques of Electron Microscopy. Biological Applications, Vol. 3. M. A. Hayat, editor. Van Nostrand Reinhold Company, New York. 113–151.

Dubochet, J., M. Ducommun, M. Zollinger, and E. Kellenberger. 1971. A new preparation method for dark-field electron microscopy of biomacromolecules. *J. Ultrastruct. Res*. 35:147–167.

Egholm, M., L. Christensen, K. L. Dueholm, O. Buchardt, J. Coull, and P. E. Nielsen. 1995. Efficient pH-independent sequence-specific DNA binding by pseudoisocytosine-containing bis-PNA. *Nucleic Acids Res.* 23:217–222.

Furrer, P., J. Bednar, A. Z. Stasiak, V. Katrich, D. Michoud, A. Stasiak, and J. Dubochet. 1997. Opposite effect of counterions on the persistence length of nicked and non-nicked DNA. *J. Mol. Biol*. 266:711–721.

Hagerman, P. J. 1988. Flexibility of DNA. *Annu. Rev. Biophys. Biophys. Chem.* 17:256–286.

Hansma, H. G., M. Bezanilla, F. Zenhausern, M. Adrian, and R. L. Sinsheimer. 1993. Atomic force microscopy of DNA in aqueous solutions. *Nucleic Acids Res.* 21:505–512.

Hansma, H. G., D. E. Laney, M. Bezanilla, R. L. Sinsheimer, and P. K. Hansma. 1995. Applications for atomic force microscopy of DNA. *Biophys. J.* 68:1672–1677.

Hansma, H. G., I. Revenko, K. Kim, and D. E. Laney. 1996. Atomic force microscopy of long and short double-stranded, single-stranded and triple-stranded nucleic acids. *Nucleic Acids Res.* 24:713–720.

Hélène, C. 1991. The anti-gene strategy: control of gene expression by triplex-forming-oligonucleotides. *Anticancer Drug Des.* 6:569–584.

Knudsen, H., and P. E. Nielsen. 1996. Antisense properties of duplex- and triplex-forming PNAs. *Nucleic Acids Res.* 24:494–500.

Kuhn, H., V. V. Demidov, M. D. Frank-Kamenetskii, and P. E. Nielsen. 1997. Sequence specificity of bis-PNAs upon targeting of double-stranded DNA. *Nucleic Acids Res.* (in press).

Larquet, E., E. Le Cam, A. Fourcade, F. Culard, P. Furrer, and E. Delain. 1996. Complémentarité des microscopies dans l'analyse de minicercles d'ADN associés à la protéine MC1. *C. R. Acad. Sci. Paris Sér. III.* 319:461–471.

Le Cam, E., F. Fack, J. Ménissier-de-Murcia, J. A. H. Cognet, A. Barbin, V. Sarantoglou, B. Révet, E. Delain, and G. de Murcia. 1994. Conformational analysis of a 139 base-pair DNA fragment containing a single-stranded break and its interaction with human poly(ADP-ribose) polymerase. *J. Mol. Biol.* 235:1062–1071.

Lee, J. S., C. Ashley, K. J. Hampel, R. Bradley, and D. G. Scraba. 1995. A stable interaction between separated pyrimidine·purine tracts in circular DNA. *J. Mol. Biol*. 252:283–288.

Lyubchenko, Yu. L., and L. S. Shlyakhtenko. 1997. Visualization of supercoiled DNA with atomic force microscopy in situ. *Proc. Natl. Acad. Sci. USA*. 94:496–501.

Møllegaard, N. E., A. I. H. Murchie, D. M. Lilley, and P. E. Nielsen. 1994. Uranyl photoprobing of a four-way DNA junction: evidence for specific metal ion binding. *Nucleic Acids Res.* 13:1508–1513.

Nielsen, P. E., M. Egholm, R. H. Berg, and O. Buchardt. 1991. Sequence selective recognition of DNA by strand displacement with a thymine-substituted polyamide. *Science.* 254:1497–1500.

Nielsen, P. E., M. Egholm, R. H. Berg, and O. Buchardt. 1993. Sequence-specific inhibition of DNA restriction enzyme cleavage by PNA. *Nucleic Acids Res.* 21:197–200.

Nielsen, P. E., M. Egholm, and O. Burchardt. 1994. Peptide nucleic acid (PNA). A DNA mimic with a peptide backbone. *Bioconjug. Chem.* 5:3–7.

Peffer, N. J., J. C. Hanvey, J. E. Bisi, S. A. Thomson, C. F. Hassman, S. A. Noble, and L. E. Babiss. 1993. Strand-invasion of duplex DNA by peptide nucleic acid oligomers. *Proc. Natl. Acad. Sci. USA*. 90: 10648–10652.

Pfannschmidt, C., A. Schapet, G. Heim, T. M. Jovin, and J. Langowski. 1996. Sequence-specific labeling of supercoiled DNA by triple-helix formation and psoralen crosslinking. *Nucleic Acids Res.* 24:1702–1709.

Schaper, A., J. P. P. Starink, and T. M. Jovin. 1994. The scanning force microscopy of DNA in air and *n*-propanol using new spreading agents. *FEBS Lett.* 355:91–95.

Svinarchuk, F., J.-R. Bertrand, and C. Malvy. 1994. A short purine oligonucleotide forms a highly stable triple helix with the promoter of the murine c-*pim*-1 proto-oncogene. *Nucleic Acids Res.* 22:3742–3747.

Svinarchuk, F., D. I. Cherny, A. Debin, E. Delain, and C. Malvy. 1996. A new approach to overcome potassium-mediated inhibition of triplex formation. *Nucleic Acids Res.* 24:3858–3865.

Svinarchuk, F., M. Monnot, A. Merle, C. Malvy, and S. Fermandjian. 1995. The high stability of the triple helices formed between short purine oligonucleotides and SIV/HIV-2 vpx genes is determined by the targeted DNA structure. *Nucleic Acids Res.* 23:3831–3836.

Thuong, N. T., and C. Hélène. 1993. Sequence-specific recognition and modification of double-helical DNA by oligonucleotides. *Angew. Chem. Int. Ed. Engl*. 32:666–690.

Wang, Y.-H., M. T. Howard, and J. D. Griffith. 1991. Phased adenine tracts in double-stranded RNA do not induce sequence-directed bending. *Biochemistry.* 30:5443–5449.